

## Characterization, pre-treatment, and potential applications of fine MSWI bottom ash as a supplementary cementitious material

Sun, Yubo; Chen, Boyu; Zhang, Shizhe; Blom, Kees; Luković, Mladena; Ye, Guang

**DOI**

[10.1016/j.conbuildmat.2024.135769](https://doi.org/10.1016/j.conbuildmat.2024.135769)

**Publication date**

2024

**Document Version**

Final published version

**Published in**

Construction and Building Materials

**Citation (APA)**

Sun, Y., Chen, B., Zhang, S., Blom, K., Luković, M., & Ye, G. (2024). Characterization, pre-treatment, and potential applications of fine MSWI bottom ash as a supplementary cementitious material. *Construction and Building Materials*, 421, Article 135769. <https://doi.org/10.1016/j.conbuildmat.2024.135769>

**Important note**

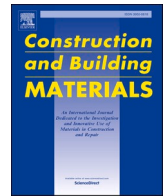
To cite this publication, please use the final published version (if applicable).  
Please check the document version above.

**Copyright**

Other than for strictly personal use, it is not permitted to download, forward or distribute the text or part of it, without the consent of the author(s) and/or copyright holder(s), unless the work is under an open content license such as Creative Commons.

**Takedown policy**

Please contact us and provide details if you believe this document breaches copyrights.  
We will remove access to the work immediately and investigate your claim.



# Characterization, pre-treatment, and potential applications of fine MSWI bottom ash as a supplementary cementitious material

Yubo Sun<sup>a,b</sup>, Boyu Chen<sup>a,\*</sup>, Shizhe Zhang<sup>a</sup>, Kees Blom<sup>c,d</sup>, Mladena Luković<sup>d</sup>, Guang Ye<sup>a,b</sup>

<sup>a</sup> *MicroLab, Section Materials and Environment, Faculty of Civil Engineering and Geosciences, Delft University of Technology, Stevinweg 1, Delft 2628 CN, the Netherlands*

<sup>b</sup> *Magnel-Vandepitte Laboratory, Department of Structural Engineering and Building Materials, Ghent University, Ghent 9052, Belgium*

<sup>c</sup> *Gemeente Rotterdam, Ingenieursbureau, the Netherlands*

<sup>d</sup> *Concrete Structures, Faculty of Civil Engineering and Geosciences, Delft University of Technology, Stevinweg 1, Delft 2628 CN, the Netherlands*

## ARTICLE INFO

### Keywords:

MSWI BA  
characterization  
pre-treatment  
metallic Al  
supplementary cementitious material

## ABSTRACT

With the development of waste recovery techniques, previous research has revealed that coarse fractions of municipal solid waste incineration (MSWI) bottom ash (BA) after proper treatment could be applied in the construction sector, while the fines are seldom recovered in practice and normally landfilled. This study explores the potential application of fine MSWI BA (0–2 mm) as a supplementary cementitious material (SCM) in Portland cement (PC) mixtures. Mechanical and chemical pre-treatment approaches have been designed with various conditions to optimize the treating process. The chemical and mineralogical compositions, as well as the metallic Al content in BA were characterized before and after the pre-treatment. It was found that both methods are effective in removing the metallic Al content in BA. Moreover, BA derived from mechanical treatment exhibited more contribution to the hydration reaction in PC mixtures, as revealed by the amount of reaction products and mineral phases formed in hardened trial mixtures. BA obtained was further partially blended in PC mortars to evaluate the performance as compared to SCMs and inert fillers. It was found that treated BA resulted in a slight retarding effect on the reaction kinetics. Treated BA behaved better than the coal fly ash to contribute to the strength development, while the inclusion of BA did not lead to significant influences on the workability.

## 1. Introduction

The rapid worldwide urbanization and industrialization over the past decades have resulted in exponential growth of waste production, which brings extensive social awareness of environmental issues [1–3]. As the most typical by-product of the urban lifestyle, it has been reported that the amount of municipal solid waste annually produced would possibly reach 2.2 billion tons per year by 2025 [4,5], leading to great pressure on waste disposal. Municipal solid waste is now directly landfilled in many regions of the world, which may introduce severe environmental impact and potential loss of resources [6–8].

With the development of more advanced waste-to-energy technology, the energy embedded in municipal solid waste might be partially recovered by generating steam and electricity through an incineration

process [9–11], which in the meantime significantly reduces the land-filling demand [12,13]. The municipal solid waste incineration (MSWI) bottom ash (BA) as the main waste stream of solid residues could be either landfilled or applied as a secondary building material [14–16]. BA obtained typically undergoes several wet treatments consisting of quenching, washing, sieving, and separating, through which the coarse unburnt particles and light organic substances are removed and sent back to the incinerator [17,18]. Metals in BA including mainly ferrous and copper are retrieved through magnet density and Eddy current separators [18]. In view of the potential application in the construction field, especially while blended in cementitious composites, previous studies [6,19] have summarized the major drawbacks as chemical barriers of MSWI BA, as shown in Table 1.

As a primary barrier limiting practical applications, the leaching

*Abbreviations:* MSWI, Municipal solid waste incineration; BA, Bottom ash; SCM, Supplementary cementitious material; PC, Portland cement; BFS, Blast furnace slag; FA, Fly ash; MQ, Micronized quartz; SEM, Scanning electron microscopy; SE, Secondary electrons; XRF, X-ray fluorescence; XRD, X-ray diffraction; STP, Standard temperature and pressure; TGA, Thermogravimetric analysis; DTG, Differential thermogravimetry; MBA, Mechanically treated BA; CBA, Chemically treated BA; LOI, Loss on ignition; Aft, Ettringite; AFm, Monosulfate.

\* Corresponding author.

E-mail address: [B.Chen-4@tudelft.nl](mailto:B.Chen-4@tudelft.nl) (B. Chen).

<https://doi.org/10.1016/j.conbuildmat.2024.135769>

Received 27 September 2023; Received in revised form 23 February 2024; Accepted 6 March 2024

Available online 11 March 2024

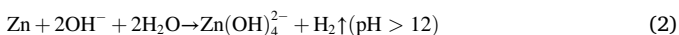
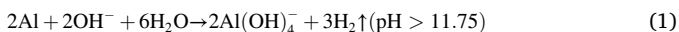
0950-0618/© 2024 The Author(s). Published by Elsevier Ltd. This is an open access article under the CC BY-NC license (<http://creativecommons.org/licenses/by-nc/4.0/>).

**Table 1**  
Major drawbacks of applying MSWI BA in cementitious composites [6,19].

Compounds in MSWI BA	Corresponding issues
Harmful salts (chloride and sulfate)	Leaching induced environmental contamination. Declined concrete durability.
Heavy metals (Cu, Zn, Cr, Ni, Mo, Pb, Sb, Au, etc.)	Leaching induced environmental contamination.
Metallic Al and Zn	Hydrogen induced cracking.

properties (including heavy metals and harmful salts) of BA have been extensively studied [20–25]. In many countries, the limit values of leaching are specified in regulations dedicated to the landfill and application of BA [26,20,24]. It has been reported that the washing treatment either with water or chemicals is efficient in mitigating the leaching of chloride and sulfate salts to meet the local requirement [27–29]. On the other hand, previous studies have proposed weathering (natural carbonation) as a promising low-cost technique to resolve the leaching of heavy metals [23–24,30], which also benefits industrial carbon capture and storage [31]. BA after quenching is normally stacked in a heap in the incineration plant, exposing to the wind and rain in under natural weather for months [32]. Due to the contact with the atmosphere air, CO<sub>2</sub> content is absorbed by hydroxides in BA to form carbonates, as Vasarevičius et al. [33] has reported a significant increase in the calcite content after the weathering process. In the meantime, calcium silicate hydrates and calcium aluminate hydrates are formed accompanied by a declined alkalinity [33,34]. A few previous studies have further explored the mechanisms of phases formed in weathered BA to immobilize the heavy metal content [6,35,36]. As a consequence, variations of the composition and properties (acid neutralizing capacity, redox potential, pH, and ion exchange capacity) lead to significant modifications in the heavy metal release characteristics of treated BA [37,38]. In EU countries, a typical natural weathering process of 6–12 weeks after quenching is commonly applied to stabilize the heavy metal and reduce leaching [34,39,13]. Accordingly, the leaching of BA could be effectively prevented through a series of proper in-plant treatments.

Previous research revealed that BA granulates obtained could partially substitute the fine and coarse aggregate in construction materials, especially in asphalt and concrete mixtures [40–43]. A few recent studies have explored certain pozzolanic reactivity of BA, which might provide an active contribution while blended with Portland cement (PC) materials [25,44–45]. It is indicated that MSWI BA could be potentially applied as a supplementary cementitious material (SCM), assisting to mitigate the environmental impact induced by the cement industry. However, the metallic Al/Zn content remains problematic while in contact with the alkaline environment in PC mixtures [46]. Hydrogen gas can be produced according to the chemical reactions expressed in Eqs. (1) and (2) [47], causing severe expansion and spalling in concrete structures [48,49].



A few treatment methods have been developed to remove the metallic Al/Zn content from MSWI BA. Several studies have proposed to submerge MSWI BA in water, where the metallic Al/Zn could be corroded by the alkalinity induced by BA itself [25,50–51]. However, this approach might be time-consuming and highly dependent on the alkali content embedded in BA [51], as Saikia et al. [52] suggested that the dissolution of metallic Al in BA initiates only when the pH in the pore solution exceeds 10. Joseph et al. [25] reported to accelerate the water treatment by using an elevated temperature of 105 °C for 24 h, while the high-temperature process is apparently more energy-intensive. Meanwhile, wet treatment with chemical substances, such as NaOH, Na<sub>2</sub>CO<sub>3</sub>, and Na<sub>2</sub>SO<sub>4</sub> solutions, has been applied to eliminate the metallic Al/Zn

through dissolution reactions [53–54,47], which appears to be more effective than the water treatment at room temperature. Moreover, a wet grinding method was proposed by Bertolini et al. [50], which deposits treated BA in slurry to remove the metallic Al/Zn content. In addition, Tang et al. [55,56] performed a series of investigations on grinding treatment combined with a high-temperature process to further improve the reactivity of BA, a 30% replacement of PC with treated BA was achieved in mortars with a 16% reduction of compressive strength. However, it remains uncertain which approach is more cost-efficient in removing the metallic Al content in MSWI BA.

Apart from that, many of the existing studies in the literature were conducted on coarser BA particles, whereas the investigation on finer fractions is still limited [6]. In addition to the general drawbacks of BA grains mentioned above, finer fractions of BA particles are normally characterized with a higher porosity, which was formed through the incineration process [57]. The porous structure in turn increases the water demand and further reduces the strength of reaction products while blended in cementitious composites [58]. In practice, the application of finer BA remains challenging to date, and they are normally discharged as sludge and directly landfilled [18,59–60].

The current study aims to perform a comprehensive investigation to characterize the fine MSWI BA and remove the embedded metallic Al content. After appropriate pre-treatment, the potential applications of treated BA as a partial substitution in cementitious materials were further explored. The BA received was first sieved into different particle fractions for characterization. Two pre-treatment methods, including mechanical and chemical approaches, were designed to remove the metallic Al/Zn content in BA. Both mechanical and chemical treating processes were optimized by varying operating conditions, and the treated BA samples were characterized again to assess the efficiency. Eventually, treated BA was blended into PC mixtures with different replacement levels to evaluate their performance as SCM and filler. The results obtained may provide a practical path for the potential application of fine MSWI BA in the construction field.

## 2. Materials and method

### 2.1. Materials

The MSWI BA particles received from the waste-to-energy company Heros Sluiskil B.V. was investigated as a potential SCM in this study. BA after incineration was water quenched, followed by proper in-plant treatments to remove the hazardous and stabilize the leachable substances [27,61–62]. Afterwards, the coarser particles were collected to produce aggregates for pavement constructions, whereas the fine fraction with a particle size of 0–2 mm as a residue was collected and used in this study to explore the potential applications.

PC CEM I 52.5 N provided by ENCI B.V. was applied as the primary cementitious material in this study. Three types of reference materials with a similar particle size distribution as PC (Fig. 1) were used in this study to assess the performance of treated BA in cementitious mixtures. Blast furnace slag (BFS) and coal fly ash (FA), as mainstream SCMs on the market, were included in comparison with the performance of treated BA to partially replace PC. BFS and FA were provided by Ecocem Benelux B.V. and Vliegasunie B.V., respectively. Besides, micronized quartz (MQ) sand was applied as a reference of inert fillers, which was provided by Sibelco Benelux B.V. Particle size distribution curves of raw materials were measured with laser diffraction by dispersing the solid particles in ethanol, as presented in Fig. 1. Results were taken as the average of five measurements. The morphology features of raw materials were visualized with a scanning electron microscopy (SEM, JEOL JSM-IT 800), as shown in Fig. 2. For each test, solid grains were uniformly stuck on a conductive tape and coated with a thin layer of platinum to improve the conductivity before visualization. The SEM images were taken under the secondary electrons (SE) mode with an accelerating voltage of 10 kV. PC, BFS, and MQ were observed with a similar

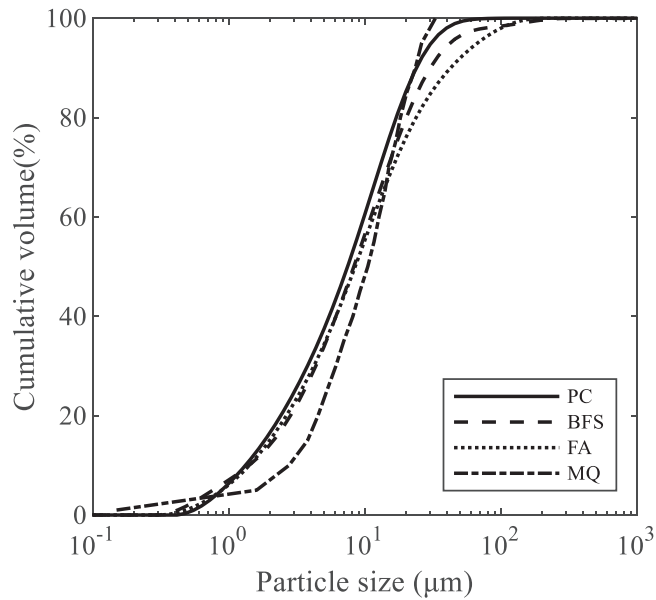


Fig. 1. Particle size distribution of raw materials used in this study.

angular-shaped microstructure, whereas spherical particles were observed in FA. In addition, CEN standard sand (according to EN 196-1 [63]) was used as the fine aggregate to prepare mortar mixtures.

Chemical compositions of the raw materials determined by X-ray fluorescence (XRF) and loss on ignition (LOI) tests, as well as their apparent density are summarized in Table 2. Lower calcium content has been detected in substitute materials compared to the CEM I 52.5 N cement. Much higher ferrous content was identified in BA compared to other raw materials. It is noteworthy that heavy metals (Cu, Pb, and Sb, etc.) were detected negligible in BA after proper in-plant treatment [18, 19]. Meanwhile, the remaining leachable salts ( $\text{Cl}^-$  and  $\text{SO}_4^{2-}$ ) in BA have reached a similar level as compared to PC. In addition, BA contains a high LOI content, which might be attributed to unburnt organic matters. Afterwards, the 0–2 mm BA received was sieved into different particle fractions for further characterizations.

## 2.2. Testing program

A flowchart of the testing program for this study is illustrated in Fig. 3, which will be explained in detail in this section.

### 2.2.1. Characterization of as-received BA

As-received BA was first characterized to assess the mechanical and chemical features of the material. In specific, the microstructure and morphology of BA was visualized with SEM by following the methods

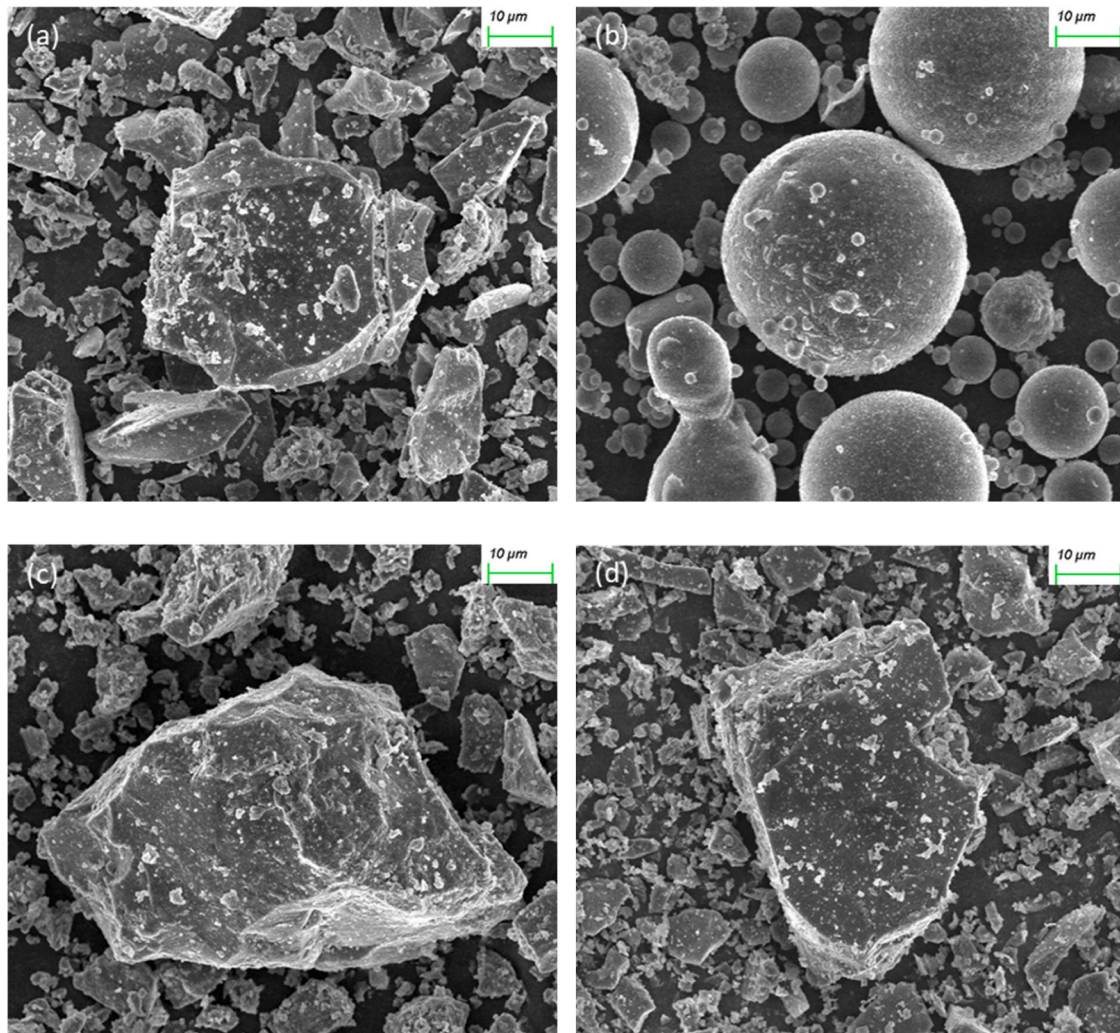


Fig. 2. Morphology of raw materials used in this study (1000×magnification, with an accelerating voltage of 10 kV) (a) PC; (b) FA; (c) BFS; (d) MQ.

**Table 2**

Chemical compositions (by mass percentage) and apparent density of raw materials used in this study.

Raw materials	CaO	SiO <sub>2</sub>	Al <sub>2</sub> O <sub>3</sub>	ZnO	MgO	SO <sub>3</sub>	Cl <sup>-</sup>	TiO <sub>2</sub>	K <sub>2</sub> O	Fe <sub>2</sub> O <sub>3</sub>	Other	LOI <sup>a</sup>	Apparent density (kg/m <sup>3</sup> )
BA (0–2 mm)	22.39	39.28	10.48	0.9	2.68	2.32	1.68	1.49	1.02	15.27	2.49	8.84	2550
PC	64.99	17.11	3.80	0.15	1.56	3.96	1.56	0.27	0.16	3.59	2.85	3.10	3160
BFS	40.90	31.10	13.48	0.19	9.16	2.31	0.31	1.26	0.69	0.40	0.2	0.10	2890
FA	3.74	56.70	24.00	0.27	1.75	1.04	0.06	1.16	2.30	6.34	2.64	2.86	2300
MQ	-	99.40	0.30	-	-	-	-	0.07	-	0.03	0.20	-	2650

<sup>a</sup> LOI measured by TG analysis at 950°C.

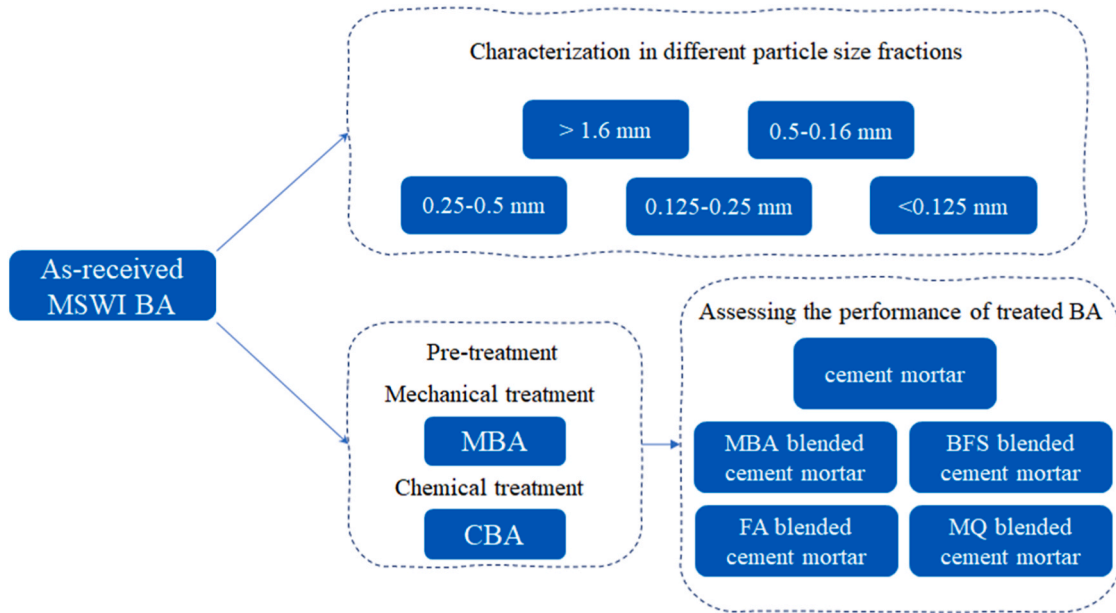


**Fig. 3.** Flowchart of the testing program for this study.

mentioned in Section 2.1. BA was then sieved into different particle fractions (<0.125 mm, 0.125–0.25 mm, 0.25–0.5 mm, 0.5–1.6 mm, and >1.6 mm) for further analysis. It is noteworthy that BA from each fraction was first ground to pass a 63 μm sieve to homogenize the material for characterization.

The chemical composition of BA from different particle fractions was first determined with XRF, while the mineralogical phases were characterized by X-ray diffraction (XRD). XRD test was conducted using a Bruker D8 Advance diffractometer with Cu-Kα radiation (λ = 1.54 Å). XRD patterns were recorded at the range between 10° and 70° with a step size of 0.02°.

Apart from that, the metallic Al/Zn content in BA samples was checked with a dissolution test [47]. As presented in Table 2, the zinc content in BA was detected below 1% according to XRF, thereby it was hypothesized that the hydrogen gas emitted from the dissolution test is ascribed to the metallic Al content. The testing device is schematically illustrated in Fig. 4. A layer of Vaseline was applied at connections to ensure air tightness.

Dissolution tests were conducted in ambient conditions (1-atmosphere pressure and temperature of 20 ± 0.5 °C). Treated BA was immersed in a 10 mol/L sodium hydroxide solution [47], where electromagnetic stirring was applied at 200 rpm for 48 h to promote the dissolution. Gases released from the reaction first went through the silica gel to remove the water vapor, and the volume of hydrogen gases collected was measured with water volume variations (Δ<sub>v</sub>) in the final cylinder. According to Eq. (1), the mass of metallic Al content, m<sub>Al</sub> (g), could be expressed with Eq. (3). Results presented in this study were determined from the average of two measurements.

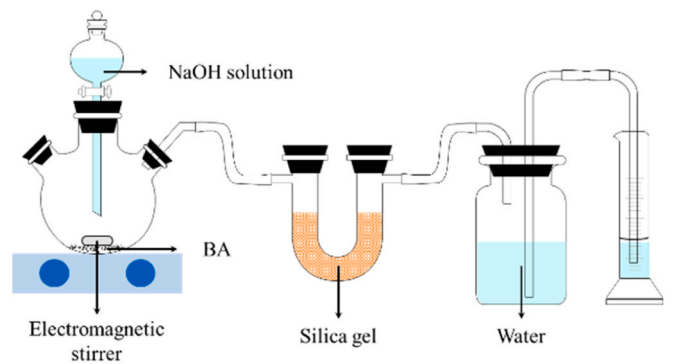


**Fig. 4.** Setup of the dissolution test to determine the metallic Al content.

$$m_{Al} = \frac{2V_{H_2}}{3V_0}M_{Al} = \frac{2\Delta V \frac{273}{273+T}}{3V_0}M_{Al} \quad (3)$$

where:

T = 20°C is the room temperature;

v<sub>0</sub> = 22.4L/mol is the molar volume at STP (Note: STP refers to the standard temperature and pressure, which is defined to be 273 K and 1-atmosphere pressure);

M<sub>Al</sub> = 27g/mol is the molar mass of Al.

### 2.2.2. Pre-treatment of BA

As aforementioned, the metallic Al/Zn content in BA would result in severe expansion and swelling while being applied as SCMs. Therefore,

pre-treatment with mechanical and chemical approaches has been performed in this study to resolve the problem.

**2.2.2.1. Mechanical treatment.** The mechanical treatment is a combined process consisting of grinding and sieving. It has been reported that the metallic Al/Zn with good ductility could be ground into metal plates and easily sieved out [55,64]. The grinding was performed with a Retsch PM100 planetary ball miller with various combinations of speed and duration to optimize grinding parameters. In specific, the grinding speed varied from 200 to 400 rpm with a 50 rpm of interval for each test. While the grinding time was selected as 10, 20, 30, and 40 min. The grinding time and speed were set according to a series of preliminary tests. The BA particles could hardly be effectively ground into fine particles to pass the sieve given a lower speed and shorter grinding time, whereas a longer duration and higher speed resulted in extremely high temperatures in the grinding jar. Afterwards, crushed BA powder was passed through a 63  $\mu\text{m}$  sieve, and the finer fraction was collected for further investigations.

**2.2.2.2. Chemical treatment.** Sodium hydroxide solutions have been prepared with different molar concentrations (0.1, 1, and 3 mol/L) to remove the metallic Al/Zn in BA [65,47,66]. BA particles were immersed in the alkaline solution with different solid to liquid ratios (0.1 and 0.2) for 5 days to assess the efficiency [53]. Treated BA particles were washed with running water and oven-dried at 105 °C until a constant mass.

**2.2.2.3. Characterization of treated BA.** Treated BA samples were characterized to evaluate the modifications made through the pre-treatment process. The chemical and mineralogical composition, as well as the remaining metallic Al content were assessed again with the method described in Section 2.2.1.

BA treated through the most effective mechanical and chemical approaches, considering both the remaining metallic Al content and the production rate (which will be addressed in detail in Section 3.2), were labeled as MBA and CBA, respectively. Extra grinding was performed on MBA and CBA to modify their particle size, ensuring a similar particle size distribution between treated BA and other raw materials. For each time, the extra grinding was conducted at 200 rpm for 1 min, and the particle size of treated BA obtained was assessed by laser diffraction tests until reaching a similar particle size distribution as indicated in Fig. 1.

The reactivity of MBA and CBA was assessed through their contribution to the hydration process, where the amount of reaction products formed in trial mixtures was determined by thermogravimetric analysis (TGA) [67]. In specific, a reference paste mixture was produced with CEM I 52.5 N cement with a water to binder (w/b) ratio of 0.5. In parallel, 10% (by mass) of cement was replaced with MBA and CBA to prepare another 2 groups of mixtures. Samples prepared with a hand-held mixer were cast into plastic molds and demolded after 24 h [68]. Hardened pastes were placed in a humid chamber (20  $\pm$  1 °C and 95% relative humidity), and the hydration reaction was terminated at the age of 28 days with solvent exchange by submerging crushed samples in anhydrous ethanol for 24 h [69,70]. The samples were then vacuum dried and ground into fine powders to pass a 63  $\mu\text{m}$  sieve. TG analysis was performed on each sample with a TG-449-F3-Jupiter instrument. For each test, about 50 mg of solid powders were incinerated in an aluminum oxide crucible from 40 to 900 °C at 10 °C/min in argon atmospheres, and the mass evolution was recorded as a function of temperature. In addition, the mineralogical phases formed in solid powders were detected by XRD with the testing method described in Section 2.2.1. TGA and XRD tests were performed twice on each sample to check the repeatability.

### 2.2.3. Application of treated BA as an SCM

**2.2.3.1. Mixture proportions.** The preliminary tests on treated BA samples indicate MBA exhibited higher reactivity over CBA. Thereby it was determined to blend MBA as a substitute material in cement mixtures to further check the effect on fresh and hardened properties. Parallel mixtures were designed to evaluate the performance of MBA comparing to mainstream SCMs and the inert quartz filler MQ, with different replacement levels (10% and 30%). Mortars were prepared according to EN 196-1 [63] with a constant w/b ratio of 0.5 and a sand to binder ratio of 3. In specific, M1 was prepared with CEM I 52.5 N as the reference mixture. M2 and M3 were designed as mixtures with MBA at a replacement level of 10% and 30%, respectively. M4 to M9 were made of other substitute materials including BFS, FA, and MQ with equivalent replacement ratios. Details of mix designs are presented in Table 3.

**2.2.3.2. Reaction kinetics.** The exothermic behavior along the hydration process was detected by a TAMAIR isothermal calorimeter on equivalent paste portions listed in Table 3. Pastes were prepared by blending solid binders and water in a Hobart planetary mixer with low speed (140 rpm) and high speed (285 rpm) for 90 s, respectively. About 14  $\pm$  0.01 g of the fresh paste after mixing was immediately loaded into a glass ampoule, which was subsequently sealed and transferred into isothermal channels of the calorimeter. The heat evolution was recorded at 20  $\pm$  0.5 °C for 100 h, and the results present in this study are normalized into 1 g of solid binder. The reaction kinetics in cement pastes were checked by the following two types of comparisons. First, the heat flow and cumulative heat release of M2 and M3 were compared to M1 to assess the influence of treated BA at different replacement ratios (10% and 30%). In addition, the effect of substituting BA with different types of SCMs and filler was evaluated at the same replacement ratio of 10% (M2, M4, M6, and M8). Calorimetry tests were performed twice to check the repeatability of results.

**2.2.3.3. Workability and strength development.** Investigations on workability and strength development were conducted on the mortar level, as presented in Table 3. Mortars were prepared with a Hobart planetary mixer. Solid components including binders, SCMs and sand were first dry-blended for 60 s. Subsequently, water was added, and the mixtures were further blended at low and high speeds for 90 s, respectively.

The workability of mortars was evaluated through the flow table test according to ASTM C1437 [71]. The mortar was filled into the conical mold in 2 layers, and each layer was compacted with a tamping rod for 20 times. After lifting the cone, 25 strokes were applied to the flow table. The spread diameter was measured and reported as the average of two measurements.

The compressive strength was tested according to EN 196-1 [63] to assess the strength development in hardened mortars. Fresh mortars after the test on workability were cast into 40  $\times$  40  $\times$  160 mm molds and vibrated for 15 seconds to release entrapped air bubbles. Mortar prisms were demolded after 24 hours and placed in a curing chamber at 20  $\pm$  1 °C with 95% relative humidity until the testing age. The compressive strength was measured at 1, 7, and 28 days, and the average strength of three specimens was reported.

## 3. Results and discussion

### 3.1. Characterization of as-received BA

The microstructural features of as-received BA were visualized by SEM, as presented in Fig. 5. Irregular-shaped BA particles embedded with extensive micro-voids and cracks have been detected, resulting in high of specific surface area and rough surface textures of BA particles. As a consequence, free water content might be entrapped in the numerous voids and pores observed, increasing the water demand to

**Table 3**  
Mix design on the mortar level.

Mix	Solid binder (g)					Water (g)	w/b	Sand (g)	Notes
	PC	MBA	BFS	FA	MQ				
M1	450	0	0	0	0	225	0.5	1350	Reference
M2	405	45	0	0	0	225	0.5	1350	10% MBA
M3	315	135	0	0	0	225	0.5	1350	30% MBA
M4	405	0	45	0	0	225	0.5	1350	10% BFS
M5	315	0	135	0	0	225	0.5	1350	30% BFS
M6	405	0	0	45	0	225	0.5	1350	10% FA
M7	315	0	0	135	0	225	0.5	1350	30% FA
M8	405	0	0	0	45	225	0.5	1350	10% MQ
M9	315	0	0	0	135	225	0.5	1350	30% MQ

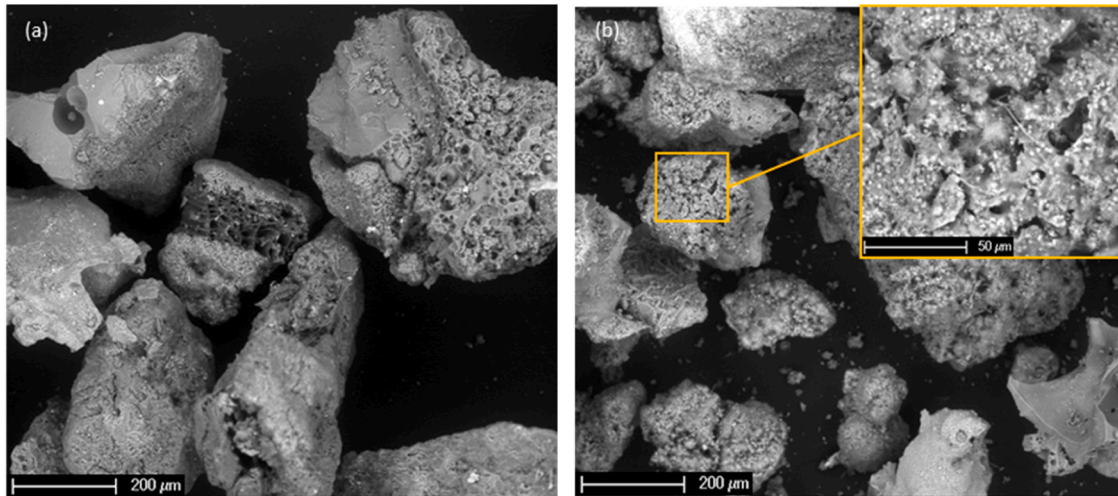


**Fig. 5.** Morphology of as-received MSWI BA (0–2 mm) detected by SEM (100 and 500×magnification, with an accelerating voltage of 10 kV).

reach a proper consistency in cementitious mixtures. Furthermore, it was found that some pores (formed through the incineration process [57]) have been interconnected and penetrated through the entire BA grain to form hollow structures. Thereby, limited mechanical properties of BA particles can be expected given the porous microstructure features [72,73].

The mass distribution derived from the sieving is presented in Table 4. It was found that the majority of as-received BA particles are distributed in the fraction between 0.5 and 1.6 mm. Besides, only a limited fraction of BA was detected with a particle size below 0.25 mm. Subsequent characterizations on as-received BA were performed on different particle fractions, separately.

The chemical compositions and metallic Al content of as-received BA samples are summarized in Table 5. It was found that the calcium and aluminum content in BA declined with the increase of particle size, while the silicate content significantly increased in coarser BA particles. In the meantime, the chloride and sulfate content, as well as LOI (mostly referring to the unburnt organics in BA) were more concentrated in smaller particle fractions. Moreover, the coarser BA fraction was detected with a higher metallic Al content.

XRD patterns of as-received BA in different particle fractions are presented in Fig. 6. A major peak located at  $26.6^\circ$  has been observed, which represents the quartz ( $\text{SiO}_2$ ) content in BA [55,74]. Apart from that, several sub-peaks referring to quartz content are distributed along

**Table 4**  
Mass of BA in different particle fractions.

Particle fraction (mm)	<0.125	0.125–0.25	0.25–0.5	0.5–1.6	>1.6
wt. (%)	2.92	3.97	13.08	45.68	34.35

XRD patterns, which is consistent with the high  $\text{SiO}_2$  content detected by XRF as shown in Table 8. In addition, calcite ( $\text{CaCO}_3$ ), Åkermanite ( $\text{Ca}_2\text{Mg}[\text{Si}_2\text{O}_7]$ ), magnetite ( $\text{Fe}_3\text{O}_4$ ) have been identified as predominant crystalline phases in BA samples, accompanied by a few crystalline peaks referring to anhydrite ( $\text{CaSO}_4$ ) and hematite ( $\text{Fe}_2\text{O}_3$ ) phases. Compared to the coarse fraction (> 1.6 mm), it is noteworthy that an amorphous hump between  $20^\circ$  and  $40^\circ$  was observed in finer fractions below 0.25 mm, which is possibly correlated to the high calcium and aluminum content in corresponding fractions as shown in Table 5. However, the amorphous humps gradually turned less apparent with the increase of BA particle sizes. In the fraction coarser than 1.6 mm, the amorphous hump was barely detected and only several highly crystalline peaks were identified.

According to the characteristics of as-received BA, it can be concluded that finer BA particles are more amorphous with less metallic Al, but contain higher chloride, sulfate, and unburnt organic matters. On the other hand, the hazardous content is less distributed in coarser particles. However, the metallic Al content is apparently increased while the particle size is greater than 0.5 mm. Thereby, it was determined to treat all BA fractions together to achieve complementary advantages.

### 3.2. Pre-treatment of BA

Treated BA was characterized again to assess the effect of different pre-treatment approaches. The metallic Al content before and after mechanical/chemical treatment was determined by the dissolution test. As-received BA contains about 0.8% metallic Al content (by mass), which is aligned with the result reported by Xuan and Poon (between 0.4% and 2.3%) [29,47]. The metallic Al content in treated BA is illustrated in Table 6 and Table 7, respectively.

**Table 5**  
Chemical compositions of as-received BA samples in different particle fractions (mass %).

Particle fraction (mm)	CaO	SiO <sub>2</sub>	Al <sub>2</sub> O <sub>3</sub>	ZnO	MgO	SO <sub>3</sub>	Cl	TiO <sub>2</sub>	K <sub>2</sub> O	Fe <sub>2</sub> O <sub>3</sub>	Other	LOI <sup>a</sup>	Metallic Al <sup>b</sup>
<0.125	38.41	16.46	15.68	1.54	2.79	4.67	2.98	2.07	1.19	11.69	2.52	12.79	0.16
0.125–0.25	35.54	25.31	11.05	1.75	2.17	3.68	2.36	1.94	1.17	13.09	1.94	9.79	0.28
0.25–0.5	36.8	21.14	10.22	2.21	2.1	4.15	2.98	1.98	1.26	14.48	2.68	8.77	0.43
0.5–1.6	21.91	39.14	11.29	0.97	2.95	2.39	1.33	1.54	1.05	16.06	1.37	7.51	1.36
>1.6	20.39	42.59	10.64	0.88	2.91	2.28	1.13	1.55	1.01	15.00	1.62	7.25	1.81

<sup>a</sup>LOI measured by TG analysis at 950 °C.

<sup>b</sup>Metallic Al content measured by the dissolution test mentioned above.

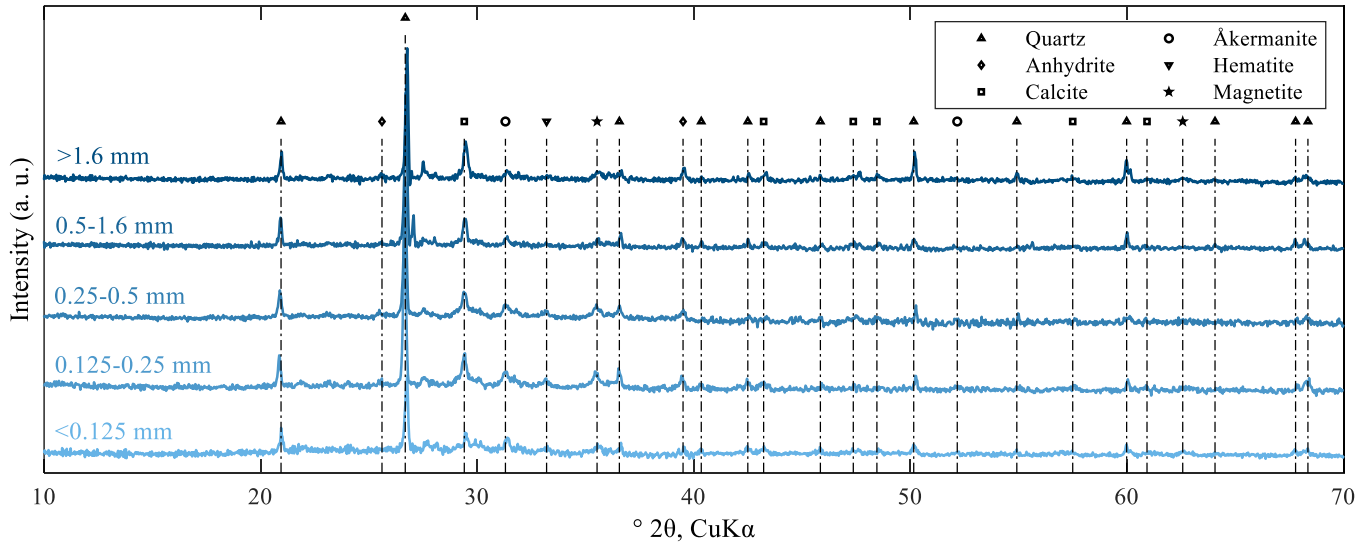


**Fig. 6.** XRD patterns of as-received BA samples from different particle fractions.

**Table 6**  
Metallic Al content (mass %) in BA after mechanical treatment.

Mechanical treatment	Grinding speed (rpm)					
	200	250	300	350	400	
Grinding time (min)	10	0.25	0.21	0.18	0.33	0.42
	20	0.22	0.19	0.15	0.43	0.67
	30	0.18	0.13	0.27	0.74	0.50
	40	0.26	0.43	0.59	0.19	0.15

**Table 7**  
Metallic Al content (mass %) in BA after chemical treatment.

Chemical treatment	Concentration of NaOH solutions (mol/L)					
	0.1	0.1	1	1	3	3
Solid/liquid (mass ratio)	0.1	0.2	0.1	0.2	0.1	0.2
Metallic Al content (mass %)	0.06	0.16	0.04	0.09	0.03	0.07

Results of mechanical treatment representing the metallic Al content in finer fractions (<63 μm) are listed in Table 6. By applying lower grinding speeds (200, 250, and 300 rpm), it was found that the remaining metallic Al content first declined but later increased with an extended grinding time. It is indicated that with a short grinding period, the metallic Al with good ductility were ground into metal plates and sieved out [55]. However, the further increase might be ascribed to that the metal plates formed were crushed into fine powders with the increase of grinding time, and thereby fell into finer fractions (as schematically illustrated in Fig. 7). In the case of higher speeds (350 and 400 rpm), the metallic Al content in finer fractions first increased, but later significantly reduced when the grinding time reached 40 min. This

is accompanied by extremely high temperatures in the grinding jar due to the intensive grinding energy applied. Results suggest that the high temperature might facilitate the oxidization of the crushed fine metallic Al powders [75], leading to a lower metallic Al content (Fig. 7).

With the scenarios illustrated in Fig. 7, both short-time & low-speed and long-time & high-speed grindings may result in a low metallic Al content in finer fractions. However, the latter approach is apparently more energy intensive. As indicated in Table 6, combinations of 200 rpm–30 min, 250 rpm–30 min, and 300 rpm–20 min were further considered due to their low residual metallic Al content. On the other hand, a less intensive grinding condition might be insufficient to crush the coarse BA particles. As a consequence, part of the BA grains might be unable to pass the sieve and separated together with the metallic plates, leading to a low production rate. Three grinding conditions mentioned above have yielded 78%, 89%, and 69% (mass percentage) of the solid to pass through the 63 μm sieve. Regarding both the residual metallic Al content and the production rate, grinding at 250 rpm for 30 min was considered as the most effective mechanical treatment approach in this study, and the treated BA derived was labeled as MBA.

As presented in Table 7, a lower solid to liquid ratio of 0.1 applied in the chemical treatment significantly reduced the remaining metallic Al content. Besides, higher NaOH dosages resulted in lower Al content after treatment. It is noteworthy that the increase in NaOH concentration from 1 to 3 mol/L did not lead to further apparent reduction, but on the other hand produced more chemical waste to be discharged. Therefore, it was determined to perform the chemical treatment by using 1 mol/L NaOH solutions with a solid/liquid ratio of 0.1 for subsequent investigations, and the BA obtained was labeled as CBA.

Compositions of BA samples are listed in Table 8. Compared to as-received BA, it can be observed that the concentration of Ca and Al slightly declined in MBA and CBA. Modifications in MBA might be correlated to the coarser particles removed by sieving, whereas the

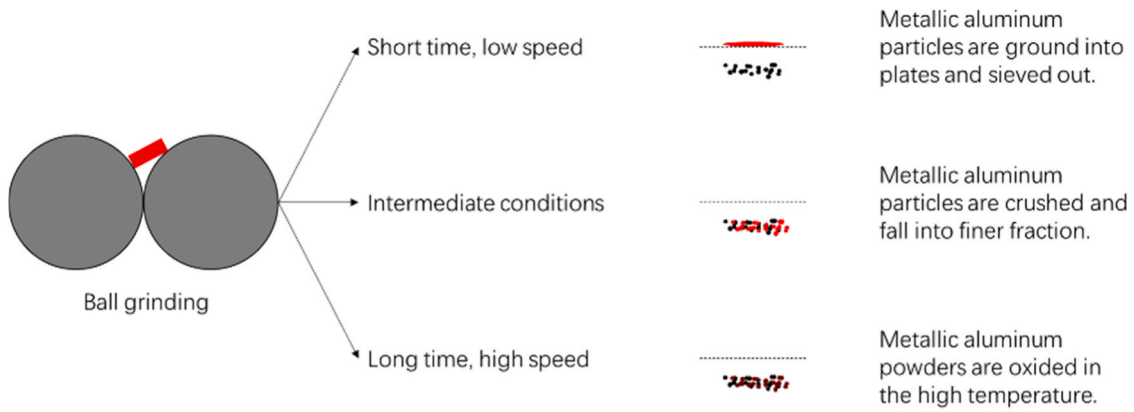


Fig. 7. Schematic sketch on grinding and sieving processes through the mechanical treatment.

**Table 8**  
Chemical compositions of as-received and treated BA samples (mass %).

	CaO	SiO <sub>2</sub>	Al <sub>2</sub> O <sub>3</sub>	ZnO	MgO	SO <sub>3</sub>	TiO <sub>2</sub>	K <sub>2</sub> O	Fe <sub>2</sub> O <sub>3</sub>	MnO	Other	LOI <sup>a</sup>	Metallic Al <sup>b</sup>
BA (0–2 mm)	22.39	39.28	10.48	0.90	2.68	2.32	1.49	1.02	15.27	2.68	1.49	8.84	0.8
MBA	21.34	46.24	10.20	0.75	2.21	0.86	1.12	0.82	13.94	1.54	0.98	4.77	0.13
CBA	19.40	50.82	9.84	0.40	2.52	0.36	1.19	0.79	11.38	2.13	1.17	2.14	0.04

<sup>a</sup>LOI measured by TG analysis at 950°C.

<sup>b</sup>Metallic Al content measured by the dissolution test mentioned above.

variation in CBA is ascribed to the compounds dissolved by the alkaline solution. Further, the remaining metallic Al content in treated BA was determined again with the dissolution test, which declined by 84% and 95% in MBA and CBA, respectively. Results have illustrated that both methods are effective in removing the metallic Al in as-received BA.

XRD patterns of BA samples are shown in Fig. 8. Results show that BA either before or after pre-treatment mainly consists of crystalline phases, whereas a slight amorphous hump was detected in BA and MBA between 20° and 40°. It is noteworthy XRD patterns of BA and MBA are nearly identical to each other, indicating that the mechanical treatment did not lead to significant phase modifications in BA samples. By contrast, the amorphous humps ranging between 20° and 40° almost disappeared in CBA, and only a few narrow crystalline peaks were detected in this region. Results suggest that a considerable amount of amorphous phases correlated to the reactive content in BA were dissolved through the chemical treatment. This can be further reflected by the reduction in the

concentration of calcium and aluminum compounds as illustrated in Table 8, which may contribute to hydration reactions in cementitious materials [76].

Afterwards, an extra grinding process was performed to further homogenize the BA samples obtained and modify the grain size. As shown in Fig. 9, the particle size distribution of MBA and CBA were kept close to that of the PC used in this study. As described in Section 2.2.2.3, MBA and CBA were then blended into trial PC mixtures with a replacement ratio of 10% to evaluate their influences on the hydration products in the hardened state. It should be noticed that the remaining metallic Al content in treated BA did not result in visible swelling or cracking in hardened samples. This will be further validated by the strength development in Section 3.3.3.

The solid powders of trial mixtures at the age of 28 days were analyzed with TGA and XRD. Mass evolution curves are plotted as a function of temperature in Fig. 10. The contribution from physically

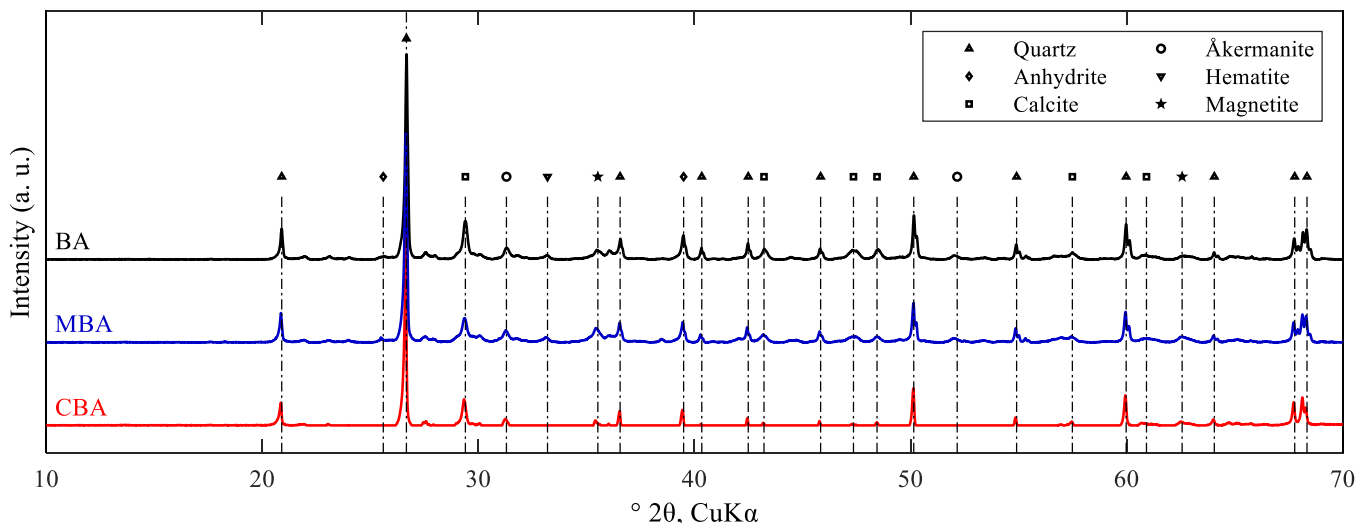


Fig. 8. XRD patterns of the as-received BA, MBA, and CBA.

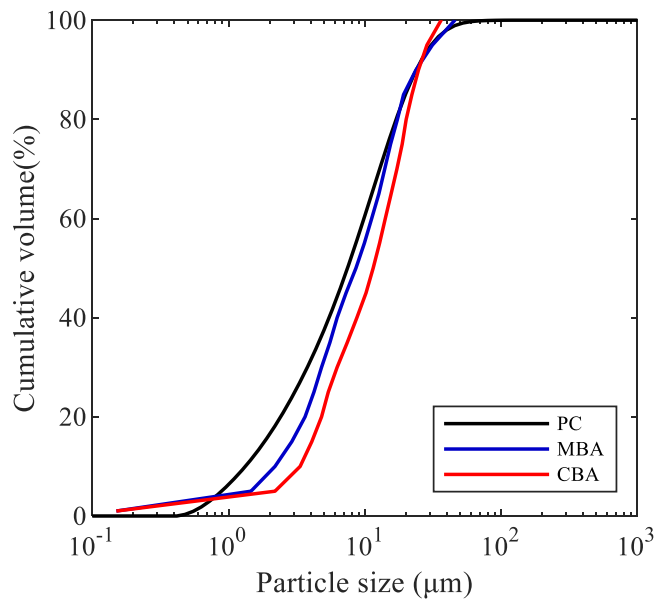


Fig. 9. Particle size distribution of PC and treated BA samples.

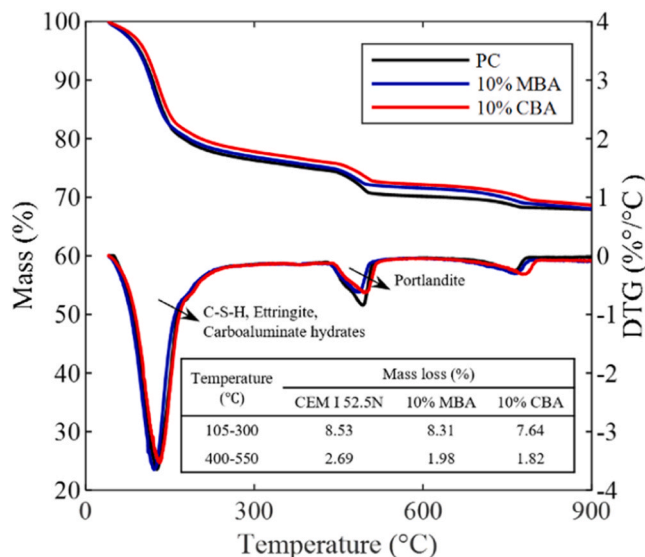


Fig. 10. TG and DTG curves of trial mixtures at the age of 28 days.

bound water is negligible through solvent exchange and vacuum preparations [77]. As shown in Fig. 10, three major peaks could be identified in differential thermogravimetry (DTG) curves. Previous studies have proposed that the first peak in DTG curve below 300 °C is attributed to a series of reactions under an elevated temperature including the water loss from C-S-H and carboaluminate hydrates [78,79], as well as the decomposition of ettringite [80] and gypsum [78]. Further, the weight loss between 440 °C and 550 °C represents the dihydroxylation of portlandite (calcium hydroxide, which is a major type of hydration product in PC) crystal into lime [81,82]. Eventually, the last peak in DTG curves located between 700 and 900 °C refers to the decomposition of calcium carbonate phases [83]. Accordingly, the mass variations in different temperature regions are also summarized in Fig. 10, assigned to different types of hydration products. Compared to the reference mix, it was found that the mass loss below 300 °C in mixtures with 10% MBA and 10% CBA was reduced by 2.6% and 10.4%, whereas the mass loss correlated to portlandite phases declined by 26.4% and 32.3% in corresponding mixtures, respectively. Results are in agreement with XRD

patterns presented in Fig. 8 that more amorphous content in CBA were dissolved through the chemical treatment, leading to less hydration products than the mixture prepared with MBA.

The mineralogical phases formed in trial mixtures at the age of 28 days are displayed in Fig. 11. Similar XRD profiles have been observed among hardened samples. Ettringite and portlandite were characterized as main reaction products, which were extensively distributed over the range of XRD patterns. Calcite phases were identified as well, with a primary peak located at around 29.3°. It was found that the intensity of peaks related to ettringite and portlandite phases slightly declined by replacing 10% PC with MBA. In the meantime, relevant crystalline phases in the sample with 10% CBA were further narrowed down, and some peaks even disappeared. Apart from that, quartz was detected in hardened mixtures with 10% MBA and 10% CBA (e.g. the peak located at 26.6°), which is correlated to the high initial quartz content in BA samples. XRD results are consistent with TG analysis. It is indicated that MBA would contribute more to the hydration process as an SCM compared to CBA.

To summarize, both mechanical and chemical treatment approaches have been employed to remove the metallic Al content in BA samples. Results indicate that both methods are efficient, and the chemical treatment has resulted in a relatively lower remaining metallic Al content after pre-treatment. In view of the potential application as SCMs, the PC mixture with MBA replacement contains a higher amount of hydration products than that prepared with the same level of CBA. It was found that the amorphous phases in BA were dissolved through the chemical treatment, and MBA exhibited more contribution to the hydration process in PC mixtures. On the other hand, the chemical treatment is more time-consuming, and resulted in high alkalinity waste chemical solutions to be discharged in practical applications. Thereby it was determined to explore further the effect of applying MBA to partially replace PC in mortar mixtures, comparing to the performances by using BFS, FA, and MQ as reference substitute materials. As shown in Fig. 12, MBA particles were detected with an angular-shaped morphology, similar to those of PC, BFS, and MQ samples (Fig. 2). The porous hollow structures with microcracks and voids of as-received BA presented in Fig. 5 were not observed after the pre-treatment. The results further indicate that the mechanical treatment has effectively declined the porosity in the BA matrix, which is also supported by the higher apparent density of MBA (2760 kg/m<sup>3</sup>) compared to that of as-received BA (2550 kg/m<sup>3</sup>) [84].

### 3.3. Application of treated BA as an SCM

#### 3.3.1. Reaction kinetics

The effect of MBA and other substitute materials on reaction kinetics was investigated with calorimetry, and results are presented in Fig. 13 and Fig. 14.

Two major peaks were observed on heat flow curves along the hydration process, as shown in Fig. 13 (a). The first peak is ascribed to the wetting and initial dissolution of cement particles once in contact with the water content [85]. Followed by the induction stage where the rate of heat release is kept at a relatively low level. The induction period lasted for about 2.5 h in the reference mixture made of pure cement. It can be observed (enlarged view in Fig. 13 (a)) that the higher the MBA replacement ratio the longer the induction period was detected. Subsequently, the onset of acceleration stage reactions was observed. In M3, the acceleration stage was initiated at about 10 h after wetting due to the high MBA content involved. As shown in Fig. 13 (a), the acceleration peak of the PC mixture consists of a main exothermic peak, accompanied by a sub-peak/shoulder located aside along the deceleration phase. It has been reported that in PC materials the main peak is attributed to the formation of C-S-H gels and crystalline portlandite phases [56], whereas the latter indicates that the calcium sulfate is consumed up, and the ettringite (AFt) formed is converted into monosulfate phases (AFm) [86–87,76]. By replacing 10% PC with MBA, it was found that the

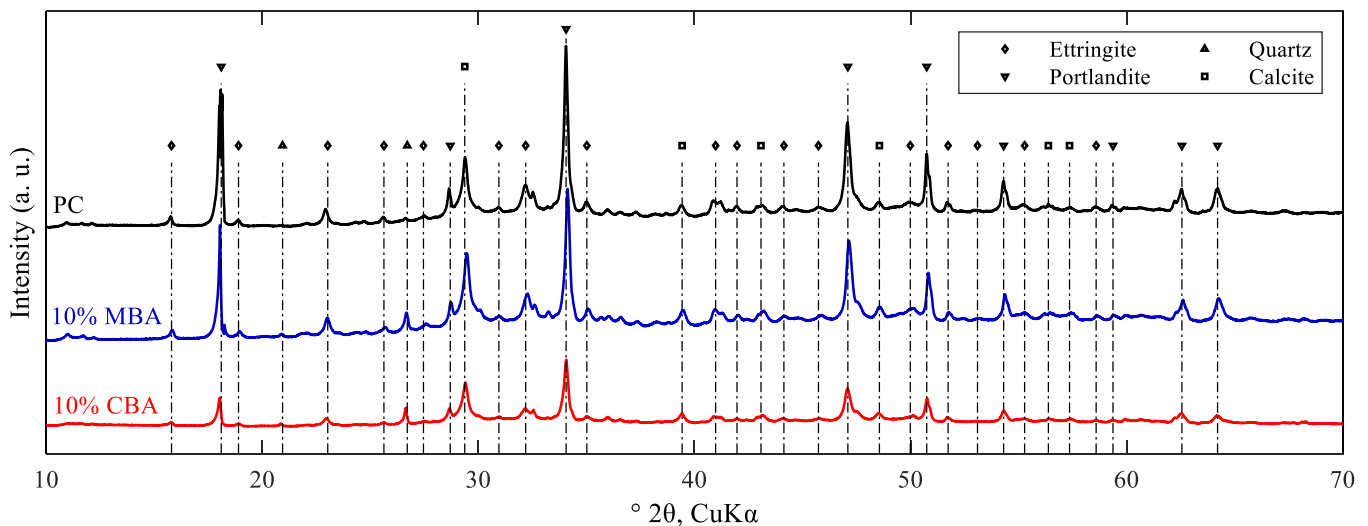


Fig. 11. XRD patterns of trail mixtures at the age of 28 days.

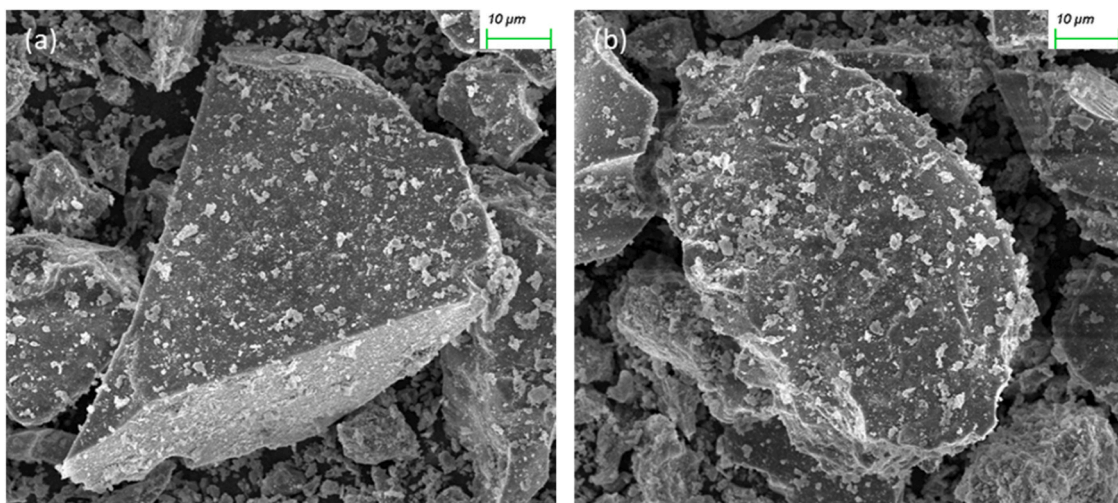


Fig. 12. Morphology of MBA particles by SEM (1000×magnification, with an accelerating voltage of 10 kV).

maximum heat flow in the former peak declined by 8.3%, while the heat flow of the shoulder referring to AFm phases was slightly reduced. In the mixture with 30% MBA, a broad shoulder occurred between 35 and 50 h (indicated with the red arrow in Fig. 13 (a)), which is consistent with results reported in previous studies [55,56]. It is indicated that the conversion from AFt to AFm phases was intensified with an increased MBA content. Meanwhile, the maximum heat flow at this stage in M2 and M3 with a higher MBA content was delayed by 1.61 and 5.32 h compared to M1, respectively. Further, the MBA content also brought certain impact on the cumulative heat release, as presented in Fig. 13 (b). Compared to M1, the cumulative heat release in M2 and M3 up to 100 h declined by 8.3% and 20.8%, respectively. Results reveal that the inclusion of MBA has led to a retarding effect on the reaction kinetics, which is possibly ascribed to the inclusion of unburnt organic content (as illustrated in Table 2) [88–90].

The effect of various substitute materials on the reaction kinetics (with a constant replacement ratio of 10%) is presented in Fig. 14. It was found that they have all resulted in less intensive exothermic behavior during the early hydration process, associated with a slight extension of the induction period. Moreover, the inclusion of substitute materials also led to reduction of cumulative heat release. Mixtures with the inert filler MQ and FA exhibited more significant reduction compared to those

prepared with BFS and MBA, indicating a less reactive nature of the substitute material during the early-stage hydration process. Up to 100 h, the cumulative heat release in M2 and M4 was decreased by about 7.5% compared to the reference mixture.

### 3.3.2. Workability

The workability of PC mixtures with different substitutes was assessed with the flow table test according to ASTM C1437 [71], as illustrated in Fig. 15. Results were taken as the average of two measurements, and it can be seen that all measurements lie within a  $\pm 10\%$  error band with respect to the average value. It is indicated that the inclusion of MBA, BFS, and MQ did not result in significant impacts on the workability of PC mixtures. This might be attributed to their similar particle size distribution and particle morphology as compared to PC (Fig. 1, Fig. 2, Fig. 9, and Fig. 12), and thereby did not result in a significant impact on the particle interactions in fresh mixtures. Partially replacing PC with FA slightly improved the spread diameter, which is ascribed to the spherical particle shape and ball-bearing effects [91,92].

### 3.3.3. Strength development

Compressive strength development of different mixtures was determined according to EN 196-1 [63] at 1, 7, and 28 days, as shown in

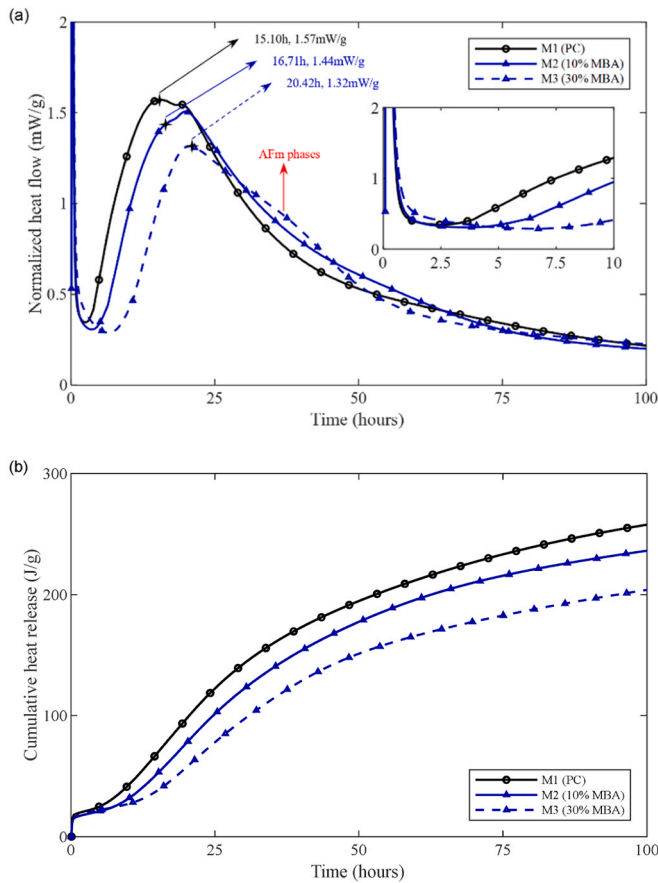


Fig. 13. Heat evolution as a function of time in mixtures with MBA at different replacement levels (a) Normalized heat flow; (b) Cumulative heat release.

Fig. 16. It should be noted that the results were taken as the average strength of three specimens, and all measurements have fallen within a  $\pm 10\%$  error band with respect to the average value. The inclusion of all substitute materials has resulted in certain reductions of strength in hardened samples. In the reference mixture, the first day compressive strength of 9.0 MPa was detected, while the 28-day strength reached 54.1 MPa. By applying 10% and 30% MBA, the 28-day strength declined by 16.7% and 35.6%, respectively. Mixtures prepared with BFS exhibited the lowest strength reductions compared to the reference mixture, indicating higher reactivity of BFS than other substitute materials. In the meantime, FA mixtures showed less strength development at early ages (1 and 7 days) compared to mixtures with the same replacement ratio of MBA. However, they have developed nearly the same level of strength after 28 days. Eventually, M8 and M9 with MQ replacement were detected with the lowest strength development among all substitute materials, since MQ content as inert fillers seldom contribute to the hydration in PC mixtures.

The first day strength development in mortar mixtures is in line with the 24-h cumulative heat release detected by calorimetry (enlarged view in Fig. 14 (b)). Moreover, it is noteworthy that the remaining metallic Al content in treated BA did not lead to significant impact on the strength development. Mixtures with MBA substitutions showed higher compressive strength than those prepared with MQ at all curing ages. It has been revealed that MBA derived in this study exhibited better performance compared to inert fillers (MQ), which could be considered as an SCM in PC mixtures. The results further illustrate that MBA may provide a better contribution to the early strength development than FA in PC mixtures, whereas the performance is still worse than that of BFS.

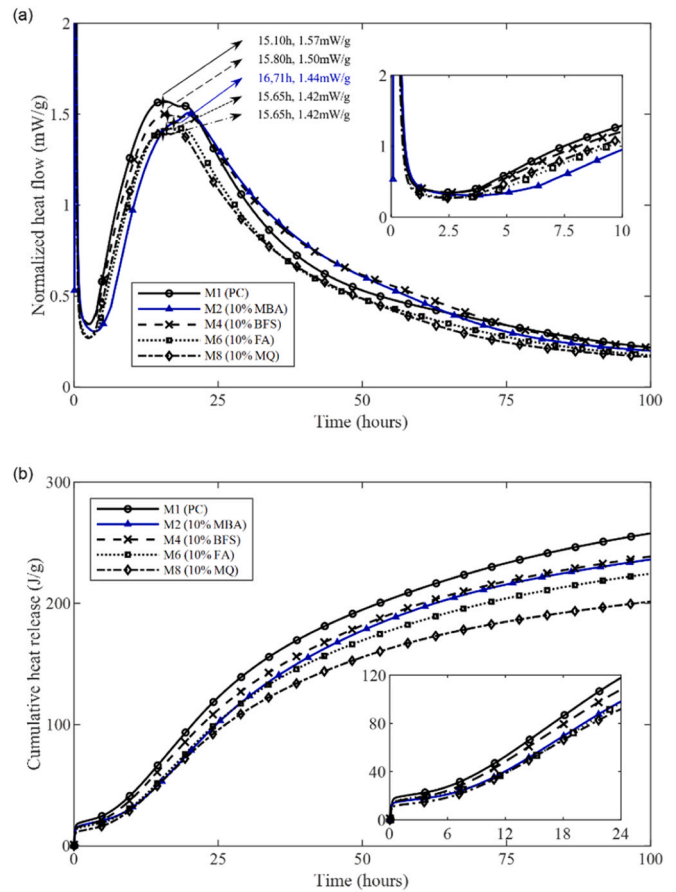


Fig. 14. Heat evolution as a function of time in mixtures with different substitute materials (a) Normalized heat flow; (b) Cumulative heat release.

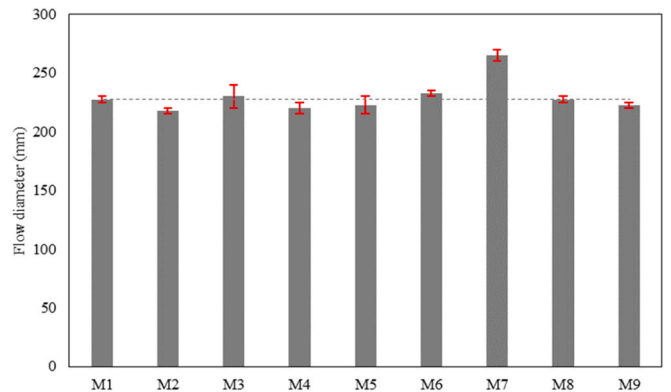
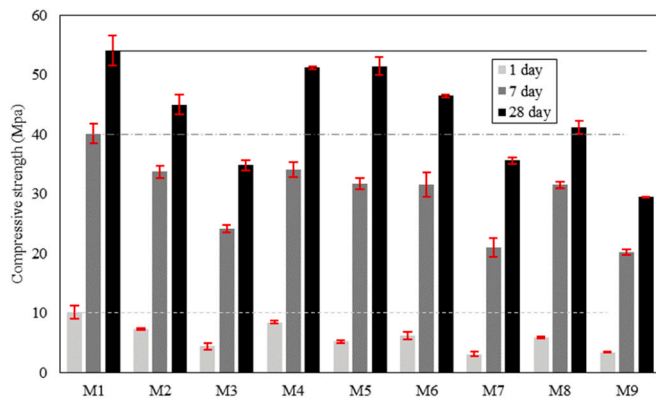


Fig. 15. Flow diameters of mortar mixtures with different substitute materials (Results were taken as the average of two measurements, the error bar represents the standard deviation).

### 3.4. Perspectives

Results presented above indicate that fine fractions of MSWI BA after the mechanical treatment proposed in this study could be potentially applied as an SCM in cementitious composites. However, it should be noted that the investigations performed remain on a laboratory scale, while more upscaling tests have to be performed to promote the industrial application of fine MSWI BA in the construction field. Moreover, the current study focused more on the characterization of BA as an SCM, while more insights into the macrostructural properties (e.g. volume stability, chemical resistance, durability, etc.) are needed in future work



**Fig. 16.** Compressive strength of mortar mixtures with different substitute materials (Results were taken as the average strength of three specimens, the error bar represents the standard deviation).

to better assess the performance of structures made of fine MSWI BA.

#### 4. Conclusions

This study attempts to explore the potential application of the fine fraction (0–2 mm) of municipal solid waste incineration (MSWI) bottom ash (BA). Different mechanical and chemical treatment approaches have been employed to reduce the metallic Al content in BA. Treated BA samples were blended in cement mixtures to assess their effects as a supplementary cementitious material (SCM) to replace Portland cement (PC). The following conclusions could be drawn according to the experimental results:

- In the 0–2 mm fraction, BA particles with a smaller grain size are more amorphous with less metallic Al, but contain higher chloride, sulfate, and unburnt organic matters. Meanwhile, the hazardous elements are less detected in BA with the increase in particle size. However, the metallic Al content in BA is apparently increased while the particle size is greater than 0.5 mm.
- The mechanical treatment was designed with low-speed grinding and sieving steps to separate the metallic Al in BA. It was detected that the remaining metallic Al content in treated BA first decreased but later increased with an extended grinding time, whereas coarser BA particles could not be crushed to pass the sieve with insufficient grinding. Grinding with 250 rpm for 30 min was considered as the most beneficial mechanical treatment approach which removed 84% of the metallic Al in BA and obtained 89% treated BA to pass through the sieve.
- High-speed grindings have resulted in high temperatures in the grinding jar, associated with the reduction in metallic Al content. This is possibly attributed to the accelerated oxidation of crushed metallic Al powders under elevated temperature conditions. However, it is more energy-consuming compared to low-speed and short-term grinding conditions.
- The chemical treatment with a sodium hydroxide solution was found to be more effective than the mechanical treatment, which reduced the metallic Al content by 95% in treated BA. However, BA after chemical treatment has led to less contribution to form hydration products in trial mixtures. The results indicate that BA after the mechanical treatment performs better as an SCM than those treated with chemical solutions.
- The inclusion of BA after mechanical treatment as partial substitution has resulted in a retarding effect on the hydration kinetics in PC mixtures. Moreover, calorimetry results suggest that the conversion from ettringite (AFt) to monosulfate (AFm) phases was intensified with an increased BA replacement ratio.

- By replacing 10% and 30% PC with BA obtained from the mechanical treatment, the 28-day compressive of hardened mortars was reduced by 16.7% and 35.6% compared to the reference mixture, respectively. Results illustrate that treated BA behaves better at early ages than the coal fly ash as an SCM to contribute to the strength development, but is still not comparable to the blast furnace slag. Further, treated BA did not lead to a significant influence on the workability of blended mixtures. It is feasible to apply treated BA obtained from this study to partially replace PC in practical applications.

#### CRediT authorship contribution statement

**Yubo Sun:** Writing – review & editing, Writing – original draft, Methodology, Investigation, Conceptualization. **Boyu Chen:** Writing – review & editing, Writing – original draft, Methodology, Investigation, Conceptualization. **Shizhe Zhang:** Writing – review & editing, Writing – original draft, Methodology, Investigation. **Kees Blom:** Writing – review & editing, Supervision, Resources, Methodology, Funding acquisition. **Mladena Luković:** Writing – review & editing, Supervision, Methodology, Investigation. **Guang Ye:** Writing – review & editing, Supervision, Methodology, Funding acquisition.

#### Declaration of Competing Interest

The authors declare that they have no known competing financial interests or personal relationships that could have appeared to influence the work reported in this paper.

#### Data Availability

Data will be made available on request.

#### Acknowledgments

The financial support from Gemeente Rotterdam for this study is gratefully acknowledged.

#### References

- [1] A. Allesch, P.H. Brunner, Assessment methods for solid waste management: a literature review, *Waste Manag. Res.* 32 (2014) 461–473.
- [2] R. Cremiato, M.L. Mastellone, C. Tagliaferri, L. Zaccariello, P. Lettieri, Environmental impact of municipal solid waste management using Life Cycle Assessment: the effect of anaerobic digestion, materials recovery and secondary fuels production, *Renew Energy* 124 (2018) 180–188.
- [3] U. Arena, M.L. Mastellone, F. Perugini, The environmental performance of alternative solid waste management options: a life cycle assessment study, *Chem. Eng. J.* 96 (2003) 207–222.
- [4] D. Hoornweg, P. Bhada-Tata, What a waste: a global review of solid waste management, (2012).
- [5] M.M. Mian, X. Zeng, A. al N.Bin Nasry, S.M.Z.F. Al-Hamadani, Municipal solid waste management in China: a comparative analysis, *J. Mater. Cycles Waste Manag.* 19 (2017) 1127–1135.
- [6] B. Chen, P. Perumal, M. Illikainen, G. Ye, A review on the utilization of municipal solid waste incineration (MSWI) bottom ash as a mineral resource for construction materials, *J. Build. Eng.* 71 (2023) 106386, <https://doi.org/10.1016/j.jobe.2023.106386>.
- [7] P. He, L. Chen, L. Shao, H. Zhang, F. Lü, Municipal solid waste (MSW) landfill: A source of microplastics?—Evidence of microplastics in landfill leachate, *Water Res* 159 (2019) 38–45.
- [8] B. Chen, Y. Zuo, S. Zhang, L.M. de Lima Junior, X. Liang, Y. Chen, M.B. van Zijl, G. Ye, Reactivity and leaching potential of municipal solid waste incineration (MSWI) bottom ash as supplementary cementitious material and precursor for alkali-activated materials, *Constr. Build. Mater.* 409 (2023) 133890.
- [9] A. Kumar, S.R. Samadder, A review on technological options of waste to energy for effective management of municipal solid waste, *Waste Manag.* 69 (2017) 407–422.
- [10] H. Cheng, Y. Hu, Municipal solid waste (MSW) as a renewable source of energy: Current and future practices in China, *Bioresour. Technol.* 101 (2010) 3816–3824.
- [11] R. Kothari, V.V. Tyagi, A. Pathak, Waste-to-energy: A way from renewable energy sources to sustainable development, *Renew. Sustain. Energy Rev.* 14 (2010) 3164–3170.
- [12] M. Li, J. Xiang, S. Hu, L.-S. Sun, S. Su, P.-S. Li, X.-X. Sun, Characterization of solid residues from municipal solid waste incinerator, *Fuel* 83 (2004) 1397–1405.

- [13] T. Sabbas, A. Poletini, R. Pomi, T. Astrup, O. Hjelm, P. Mostbauer, G. Cappai, G. Magel, S. Salhofer, C. Speiser, Management of municipal solid waste incineration residues, *Waste Manag.* 23 (2003) 61–88.
- [14] M. Van Praagh, M. Johansson, J. Fagerqvist, R. Grönholm, N. Hansson, H. Svensson, Recycling of MSWI-bottom ash in paved constructions in Sweden—A risk assessment, *Waste Manag.* 79 (2018) 428–434.
- [15] A. Vaitkus, J. Gražulytė, O. Šernas, V. Vorobjovas, R. Kleizienė, An algorithm for the use of MSWI bottom ash as a building material in road pavement structural layers, *Constr. Build. Mater.* 212 (2019) 456–466.
- [16] W.-B. Li, J. Yao, Z. Malik, G.-D. Zhou, M. Dong, D.-S. Shen, Impact of MSWI bottom ash codisposed with MSW on landfill stabilization with different operational modes, *Biomed. Res. Int.* 2014 (2014).
- [17] O. Ginés, J.M. Chimenos, A. Vizcarro, J. Formosa, J.R. Rosell, Combined use of MSWI bottom ash and fly ash as aggregate in concrete formulation: Environmental and mechanical considerations, *J. Hazard. Mater.* 169 (2009) 643–650.
- [18] C. Vandecasteele, Integrated municipal solid waste treatment using a grate furnace incinerator, *Indaver case 27* (2007) 1366–1375, <https://doi.org/10.1016/j.wasman.2006.08.005>.
- [19] B. Verbinen, P. Billen, J. Van Caneghem, C. Vandecasteele, Recycling of MSWI Bottom Ash: A Review of Chemical Barriers, Engineering Applications and Treatment Technologies, *Waste Biomass.-. Valoriz.* 8 (2017) 1453–1466, <https://doi.org/10.1007/s12649-016-9704-0>.
- [20] O. Hjelm, J. Holm, K. Crillessen, Utilisation of MSWI bottom ash as sub-base in road construction: first results from a large-scale test site, *J. Hazard. Mater.* 139 (2007) 471–480.
- [21] S. Olsson, E. Kärrman, J.P. Gustafsson, Environmental systems analysis of the use of bottom ash from incineration of municipal waste for road construction, *Resour. Conserv. Recycl.* 48 (2006) 26–40.
- [22] L. Su, G. Guo, X. Shi, M. Zuo, D. Niu, A. Zhao, Y. Zhao, Copper leaching of MSWI bottom ash co-disposed with refuse: effect of short-term accelerated weathering, *Waste Manag.* 33 (2013) 1411–1417.
- [23] Y. Hu, L. Zhao, Y. Zhu, B. Zhang, G. Hu, B. Xu, C. He, F. Di Maio, The fate of heavy metals and salts during the wet treatment of municipal solid waste incineration bottom ash, *Waste Manag.* 121 (2021) 33–41.
- [24] T. Van Gerven, E. Van Keer, S. Aricx, M. Jaspers, G. Wauters, C. Vandecasteele, Carbonation of MSWI-bottom ash to decrease heavy metal leaching, in view of recycling, *Waste Manag.* 25 (2005) 291–300.
- [25] A.M. Joseph, R. Snellings, P. Nielsen, S. Matthys, N. De, Belie, Pre-treatment and utilisation of municipal solid waste incineration bottom ashes towards a circular economy, *Constr. Build. Mater.* 260 (2020) 120485.
- [26] I. Vateva, D. Laner, Grain-size specific characterisation and resource potentials of municipal solid waste incineration (MSWI) bottom ash: A German case study, *Resources* 9 (2020) 66.
- [27] A. Keulen, A. van Zomeren, P. Harpe, W. Aarnink, H.A.E. Simons, H.J.H. Brouwers, High performance of treated and washed MSWI bottom ash granulates as natural aggregate replacement within earth-moist concrete, *Waste Manag.* 49 (2016) 83–95.
- [28] Q. Alam, M.V.A. Florea, K. Schollbach, H.J.H. Brouwers, A two-stage treatment for Municipal Solid Waste Incineration (MSWI) bottom ash to remove agglomerated fine particles and leachable contaminants, *Waste Manag.* 67 (2017) 181–192.
- [29] D. Xuan, P. Tang, C.S. Poon, Limitations and quality upgrading techniques for utilization of MSW incineration bottom ash in engineering applications—A review, *Constr. Build. Mater.* 190 (2018) 1091–1102.
- [30] S. Aricx, V. De Borger, T. Van Gerven, C. Vandecasteele, Effect of carbonation on the leaching of organic carbon and of copper from MSWI bottom ash, *Waste Manag.* 30 (2010) 1296–1302.
- [31] R.M. Santos, G. Mertens, M. Salman, Ö. Cizer, T. Van Gerven, Comparative study of ageing, heat treatment and accelerated carbonation for stabilization of municipal solid waste incineration bottom ash in view of reducing regulated heavy metal/metalloid leaching, *J. Environ. Manag.* 128 (2013) 807–821.
- [32] E. Allegrini, A. Maresca, M.E. Olsson, M.S. Holtze, A. Boldrin, T.F. Astrup, Quantification of the resource recovery potential of municipal solid waste incineration bottom ashes, *Waste Manag.* 34 (2014) 1627–1636.
- [33] S. Vasarevičius, J. Seniūnaitė, V. Vaišis, Impact of natural weathering on stabilization of heavy metals (Cu, Zn, and Pb) in MSWI bottom ash, *Appl. Sci.* 12 (2022) 3419.
- [34] M. Gori, B. Bergfeldt, G. Pfrang-Stotz, J. Reichelt, P. Sirini, Effect of short-term natural weathering on MSWI and wood waste bottom ash leaching behaviour, *J. Hazard. Mater.* 189 (2011) 435–443.
- [35] J. Chen, Y. Shen, Z. Chen, C. Fu, M. Li, T. Mao, R. Xu, X. Lin, X. Li, J. Yan, Accelerated carbonation of ball-milling modified MSWI fly ash: Migration and stabilization of heavy metals, *J. Environ. Chem. Eng.* 11 (2023) 109396.
- [36] A. Maldonado-Alameda, J. Giro-Paloma, A. Rodríguez-Romero, J. Serret, A. Menargues, A. Andrés, J.M. Chimenos, Environmental potential assessment of MSWI bottom ash-based alkali-activated binders, *J. Hazard. Mater.* 416 (2021) 125828.
- [37] L. Su, S. Wang, R. Ji, G. Zhuo, C. Liu, M. Chen, H. Li, L. Zhang, New insight into the role of FDOM in heavy metal leaching behavior from MSWI bottom ash during accelerated weathering using fluorescence EEM-PARAFAC, *Waste Manag.* 144 (2022) 153–162.
- [38] A. Poletini, R. Pomi, The leaching behavior of incinerator bottom ash as affected by accelerated ageing, *J. Hazard. Mater.* 113 (2004) 209–215.
- [39] A. Maldonado-Alameda, J. Giro-Paloma, F. Andreola, L. Barbieri, J.M. Chimenos, I. Lancellotti, Weathered bottom ash from municipal solid waste incineration: Alkaline activation for sustainable binders, *Constr. Build. Mater.* 327 (2022) 126983, <https://doi.org/10.1016/j.conbuildmat.2022.126983>.
- [40] R. Forteza, M. Far, C. Segui, V. Cerdá, Characterization of bottom ash in municipal solid waste incinerators for its use in road base, *Waste Manag.* 24 (2004) 899–909.
- [41] U. Müller, K. Rübner, The microstructure of concrete made with municipal waste incinerator bottom ash as an aggregate component, *Cem. Concr. Res.* 36 (2006) 1434–1443.
- [42] J. Lu, X. Yang, Y. Lai, X. Wan, J. Gao, Y. Wang, L. Tan, F. Deng, Utilization of municipal solid waste incinerator bottom ash (MSWIBA) in concrete as partial replacement of fine aggregate, *Constr. Build. Mater.* 414 (2024) 134918.
- [43] J. Gražulytė, A. Vaitkus, O. Šernas, L. Žalimienė, The impact of MSWI bottom ash as aggregate on concrete mechanical performance, *Int. J. Pavement Eng.* 23 (2022) 2903–2911.
- [44] F. Faleschini, K. Toska, M.A. Zanini, F. Andreose, A.G. Settimi, K. Brunelli, C. Pellegrino, Assessment of a Municipal Solid Waste Incinerator Bottom Ash as a Candidate Pozzolanic Material: Comparison of Test Methods, *Sustainability* 13 (2021) 8998.
- [45] S. Zhang, Z. Ghoulou, Z. He, L. Hu, Y. Shao, Use of municipal solid waste incineration bottom ash as a supplementary cementitious material in dry-cast concrete, *Constr. Build. Mater.* 266 (2021) 120890.
- [46] A. Taherlou, G. Asadollahfardi, A.M. Salehi, A. Katebi, Sustainable use of municipal solid waste incinerator bottom ash and the treated industrial wastewater in self-compacting concrete, *Constr. Build. Mater.* 297 (2021) 123814.
- [47] D. Xuan, C.S. Poon, Removal of metallic Al and Al/Zn alloys in MSWI bottom ash by alkaline treatment, *J. Hazard. Mater.* 344 (2018) 73–80, <https://doi.org/10.1016/j.jhazmat.2017.10.002>.
- [48] K. Rübner, F. Haamkens, O. Linde, Use of municipal solid waste incinerator bottom ash as aggregate in concrete, *Q. J. Eng. Geol. Hydrogeol.* 41 (2008) 459–464.
- [49] J.K. Magnuson, K.D. Weiksnar, A.D. Patel, K.A. Clavier, C.C. Ferraro, T. G. Townsend, Processing municipal solid waste incineration bottom ash for integration into cement product manufacture, *Resour. Conserv. Recycl.* 198 (2023) 107139.
- [50] L. Bertolini, M. Carsana, D. Cassago, A.Q. Curzio, M. Collepardi, MSWI ashes as mineral additions in concrete, *Cem. Concr. Res.* 34 (2004) 1899–1906.
- [51] B. Chen, G. Ye, The role of water-treated municipal solid waste incineration (MSWI) bottom ash in microstructure formation and strength development of blended cement pastes, *Cem. Concr. Res.* 178 (2024) 107440.
- [52] N. Saikia, G. Mertens, K. Van Balen, J. Elsen, T. Van Gerven, C. Vandecasteele, Pre-treatment of municipal solid waste incineration (MSWI) bottom ash for utilisation in cement mortar, *Constr. Build. Mater.* 96 (2015) 76–85, <https://doi.org/10.1016/j.conbuildmat.2015.07.185>.
- [53] R.P. Penilla, A.G. Bustos, S.G. Elizabale, Zeolite synthesized by alkaline hydrothermal treatment of bottom ash from combustion of municipal solid wastes, *J. Am. Ceram. Soc.* 86 (2003) 1527–1533, <https://doi.org/10.1111/j.1151-2916.2003.tb03509.x>.
- [54] J. Bawab, J. Khatib, S. Kenai, M. Sonebi, A review on cementitious materials including municipal solid waste incineration bottom ash (MSWI-BA) as aggregates, *Buildings* 11 (2021) 179.
- [55] P. Tang, M.V.A. Florea, P. Spiesz, H.J.H. Brouwers, Application of thermally activated municipal solid waste incineration (MSWI) bottom ash fines as binder substitute, *Cem. Concr. Compos.* 70 (2016) 194–205, <https://doi.org/10.1016/j.cemconcomp.2016.03.015>.
- [56] P. Tang, W. Chen, D. Xuan, Y. Zuo, C.S. Poon, Investigation of cementitious properties of different constituents in municipal solid waste incineration bottom ash as supplementary cementitious materials, *J. Clean. Prod.* 258 (2020) 120675.
- [57] A.P. Bayuseno, W.W. Schmahl, Understanding the chemical and mineralogical properties of the inorganic portion of MSWI bottom ash, *Waste Manag.* 30 (2010) 1509–1520, <https://doi.org/10.1016/j.wasman.2010.03.010>.
- [58] E. Loginova, K. Schollbach, M. Proskurnin, H.J.H. Brouwers, Municipal solid waste incineration bottom ash fines: Transformation into a minor additional constituent for cements, *Resour. Conserv. Recycl.* 166 (2021) 105354.
- [59] Y. Cheng, G. Gao, L. Chen, W. Du, W. Mu, Y. Yan, H. Sun, Physical and mechanical study of municipal solid waste incineration (MSWI) bottom ash with different particle size distribution, *Constr. Build. Mater.* 416 (2024) 135137.
- [60] S. Keber, T. Schirmer, T. Elwert, D. Goldmann, Characterization of fine fractions from the processing of municipal solid waste incinerator bottom ashes for the potential recovery of valuable metals, *Minerals* 10 (2020) 838.
- [61] Y.-C. Lin, S.C. Panchangam, C.-H. Wu, P.-K.A. Hong, C.-F. Lin, Effects of water washing on removing organic residues in bottom ashes of municipal solid waste incinerators, *Chemosphere* 82 (2011) 502–506.
- [62] S. Aricx, T. Van Gerven, C. Vandecasteele, Accelerated carbonation for treatment of MSWI bottom ash, *J. Hazard. Mater.* 137 (2006) 235–243.
- [63] T.S. EN, 196-1, Methods of testing cement—Part 1: Determination of strength, *Eur. Comm. Stand* 26 (2005).
- [64] B. Chen, J. Chen, F.F. de Mendonça Filho, Y. Sun, M.B. van Zijl, O. Copuroglu, G. Ye, Characterization and mechanical removal of metallic aluminum (Al) embedded in weathered municipal solid waste incineration (MSWI) bottom ash for application as supplementary cementitious material, *Waste Manag.* 176 (2024) 128–139.
- [65] J.E. Aubert, B. Husson, N. Sarracone, Utilization of municipal solid waste incineration (MSWI) fly ash in blended cement. Part 2. Mechanical strength of mortars and environmental impact, *J. Hazard. Mater.* 146 (2007) 12–19, <https://doi.org/10.1016/j.jhazmat.2006.11.044>.
- [66] J. Pera, L. Coutaz, J. Ambroise, M. Chababbet, Use of incinerator bottom ash in concrete, *Cem. Concr. Res.* 27 (1997) 1–5.
- [67] A. Choudhary, K. Bharadwaj, R.M. Ghantous, O.B. Isgor, W.J. Weiss, Pozzolanic Reactivity Test of Supplementary Cementitious Materials, *Acids Mater. J.* 119 (2022).

- [68] A. Tironi, M.A. Trezza, A.N. Scian, E.F. Irassar, Cement & Concrete Composites Assessment of pozzolanic activity of different calcined clays, *Cem. Concr. Compos* 37 (2013) 319–327, <https://doi.org/10.1016/j.cemconcomp.2013.01.002>.
- [69] J. Zhang, G.W. Scherer, Cement and Concrete Research Comparison of methods for arresting hydration of cement, *Cem. Concr. Res* 41 (2011) 1024–1036, <https://doi.org/10.1016/j.cemconres.2011.06.003>.
- [70] D.H. Bager, E.J. Sellevold, How to prepare polished cement product surfaces for optical microscopy without introducing visible cracks, *Cem. Concr. Res.* 9 (1979) 653–654.
- [71] A. C1437, Standard test method for flow of hydraulic cement mortar, Philadelphia, PA. (2001).
- [72] L. Andrade, J.C. Rocha, M. Cheriaf, Evaluation of concrete incorporating bottom ash as a natural aggregates replacement, *Waste Manag.* 27 (2007) 1190–1199.
- [73] P. Tang, M.V.A. Florea, P. Spiesz, H.J.H. Brouwers, Characteristics and application potential of municipal solid waste incineration (MSWI) bottom ashes from two waste-to-energy plants, *Constr. Build. Mater.* 83 (2015) 77–94.
- [74] X.C. Qiao, M. Tyrer, C.S. Poon, C.R. Cheeseman, Novel cementitious materials produced from incinerator bottom ash, *Resour. Conserv. Recycl.* 52 (2008) 496–510, <https://doi.org/10.1016/j.resconrec.2007.06.003>.
- [75] D.R. Clarke, Stress generation during high-temperature oxidation of metallic alloys, *Curr. Opin. Solid State Mater. Sci.* 6 (2002) 237–244.
- [76] J.W. Bullard, H.M. Jennings, R.A. Livingston, A. Nonat, G.W. Scherer, J. S. Schweitzer, K.L. Scrivener, J.J. Thomas, Mechanisms of cement hydration, *Cem. Concr. Res.* 41 (2011) 1208–1223.
- [77] S. Zhang, Z. Li, B. Ghiassi, S. Yin, G. Ye, Fracture properties and microstructure formation of hardened alkali-activated slag/fly ash pastes, *Cem. Concr. Res.* 144 (2021) 106447.
- [78] L. Alarcon-Ruiz, G. Platret, E. Massieu, A. Ehrlacher, The use of thermal analysis in assessing the effect of temperature on a cement paste, *Cem. Concr. Res.* 35 (2005) 609–613, <https://doi.org/10.1016/j.cemconres.2004.06.015>.
- [79] G.A. Khoury, Compressive strength of concrete at high temperatures: a reassessment, *Mag. Concr. Res.* 44 (1992) 291–309.
- [80] Q. Zhou, F.P. Glasser, Thermal stability and decomposition mechanisms of ettringite at <math>120^{\circ}\text{C}</math>, *Cem. Concr. Res.* 31 (2001) 1333–1339, [https://doi.org/10.1016/S0008-8846\(01\)00558-0](https://doi.org/10.1016/S0008-8846(01)00558-0).
- [81] D. Thermal, M. Of, E. Calcium, H. In, C. Silicate, C. Pastes, ( Communicated by P. J. Sereida), 9 (1979) 677–684.
- [82] L. Franke, K. Sisomphon, A new chemical method for analyzing free calcium hydroxide content in cementing material 34 (2004) 1161–1165, <https://doi.org/10.1016/j.cemconres.2003.12.003>.
- [83] P.E. Grattan-Bellew, Microstructural investigation of deteriorated Portland cement concretes, *Constr. Build. Mater.* 10 (1996) 3–16, [https://doi.org/10.1016/0950-0618\(95\)00066-6](https://doi.org/10.1016/0950-0618(95)00066-6).
- [84] M. Heikal, Effect of temperature on the physico-mechanical and mineralogical properties of Homra pozzolanic cement pastes, *Cem. Concr. Res.* 30 (2000) 1835–1839.
- [85] N.Y. Mostafa, P.W. Brown, Heat of hydration of high reactive pozzolans in blended cements, *Isothermal Conduct. Calorim.* 435 (2005) 162–167, <https://doi.org/10.1016/j.tca.2005.05.014>.
- [86] D. Jansen, F. Goetz-Neunhoeffer, B. Lothenbach, J. Neubauer, The early hydration of Ordinary Portland Cement (OPC): an approach comparing measured heat flow with calculated heat flow from QXRD, *Cem. Concr. Res.* 42 (2012) 134–138.
- [87] K. Scrivener, A. Ouzia, P. Juilland, A.K. Mohamed, Advances in understanding cement hydration mechanisms, *Cem. Concr. Res.* 124 (2019) 105823.
- [88] H. Shi, L. Kan, Characteristics of municipal solid wastes incineration (MSWI) fly ash–cement matrices and effect of mineral admixtures on composite system, *Constr. Build. Mater.* 23 (2009) 2160–2166.
- [89] N. Gineys, G. Aouad, D. Damidot, Managing trace elements in Portland cement–Part I: Interactions between cement paste and heavy metals added during mixing as soluble salts, *Cem. Concr. Compos.* 32 (2010) 563–570.
- [90] C. Medina, P.F.G. Banfill, M.I.S. De Rojas, M. Frías, Rheological and calorimetric behaviour of cements blended with containing ceramic sanitary ware and construction/demolition waste, *Constr. Build. Mater.* 40 (2013) 822–831.
- [91] T. Yang, H. Zhu, Z. Zhang, X. Gao, C. Zhang, Q. Wu, Effect of fly ash microsphere on the rheology and microstructure of alkali-activated fly ash/slag pastes, *Cem. Concr. Res.* 109 (2018) 198–207, <https://doi.org/10.1016/j.cemconres.2018.04.008>.
- [92] Y.-Y. Chen, B.L.A. Tuan, C.-L. Hwang, Effect of paste amount on the properties of self-consolidating concrete containing fly ash and slag, *Constr. Build. Mater.* 47 (2013) 340–346.